Broken Ring Speciation in California Mygalomorph Spiders (Nemesiidae, *Calisoga*)

Rodrigo Monjaraz-Ruedas,[1,*] James Starrett,[2] Dean Leavitt,[3] and Marshal Hedin[1]

1. Department of Biology, San Diego State University, San Diego, California 92182; 2. Department of Entomology and Nematology, University of California, Davis, California 95616; 3. Department of Biology, San Diego Mesa College, San Diego, California 92111

Submitted October 18, 2023; Accepted February 19, 2024; Electronically published May 22, 2024

Online enhancements: supplemental PDF, tables.

ABSTRACT: Idealized ring species, with approximately continuous gene flow around a geographic barrier but singular reproductive isolation at a ring terminus, are rare in nature. A broken ring species model preserves the geographic setting and fundamental features of an idealized model but accommodates varying degrees of gene flow restriction over complex landscapes through evolutionary time. Here we examine broken ring species dynamics in *Calisoga* spiders, which, like the classic ring species *Ensatina* salamanders, are distributed around the Central Valley of California. Using nuclear and mitogenomic data, we test key predictions of common ancestry, ringlike biogeography, biogeographic timing, population connectivity, and terminal overlap. We show that a ring complex of populations shares a single common ancestor, and from an ancestral area in the Sierra Nevada mountains, two distributional and phylogenomic arms encircle the Central Valley. Isolation by distance occurs along these distributional arms, although gene flow restriction is also evident. Where divergent lineages meet in the South Coast Ranges, we find rare lineage sympatry, without evidence for nuclear gene flow and with clear evidence for morphological and ecological divergence. We discuss general insights provided by broken ring species and how such a model could be explored and extended in other systems and future studies.

Keywords: biogeography, evolutionary persistence, gene flow, isolation by distance, parapatry.

Introduction

In "idealized" ring speciation, an ancestral population disperses around a central geographic barrier, creating an approximately continuous chain of populations interconnected by genetic exchange (Mayr 1942; Stebbins 1949; Irwin et al. 2001; Cacho and Baum 2012; Irwin and Wake 2016; Kuchta and Wake 2016). When populations meet at the barrier terminus, they have accumulated enough genetic and phenotypic differences to prevent substantial gene flow, resulting in two distinct species under a classic biological species concept. Ring species are interesting to evolutionary biologists in illustrating a link between micro- and macroevolution, with geographic space serving as a proxy for evolutionary time. Ring species also provide insight into divergence with gene flow and showcase speciation completion dynamics at a ring terminus (Irwin et al. 2001; Pereira et al. 2011; Alcaide et al. 2014; Irwin and Wake 2016; Kuchta and Wake 2016). Finally, ring species provide system-specific biogeographic details but also general insight into the nature of dispersal corridors and barriers to dispersal (Monahan et al. 2012).

Idealized ring species are extremely rare and, with continued genomic scrutiny or strict definitions, perhaps do not exist in nature. Continuous gene flow throughout an entire lineage history is difficult to achieve, dependent on organismal biology (population sizes, dispersal abilities), habitat continuity, climatic variation through time, and local population extinction (Irwin et al. 2001; Alcaide et al. 2014; Irwin and Wake 2016; Kuchta and Wake 2016). Also, terminal contact may not have been discovered, may not exist (Irwin et al. 2001; Rubinoff et al. 2021), or may allow for extensive gene flow (Alcaide et al. 2014; Bouzid et al. 2022). Simulation studies support the contention that idealized ring species should be rare in nature, requiring a specific combination of evolutionary age, dispersal rate, carrying capacity, and geographic configuration (Martins et al. 2013).

These empirical and theoretical challenges do not diminish the importance or interest in ringlike dynamics (Kuchta and Wake 2016). The key processes of a ring model (divergence with gene flow, space as a surrogate for time, ring terminus interactions) may still exist in different spatial regions of a ring complex or may have existed historically, even if not achieved simultaneously at present. Recognizing

* Corresponding author; email: monroderik@gmail.com.

ORCIDs: Monjaraz-Ruedas, https://orcid.org/0000-0002-6462-3739; Leavitt, https://orcid.org/0000-0002-9311-5522; Hedin, https://orcid.org/0000-0001-7683-9572.

  https://doi.org/10.1086/730262

that an idealized model is empirically unrealistic, Irwin and Wake (2016) and Kuchta and Wake (2016) present arguments for less restrictive ring speciation models. These allow for varying degrees of population fragmentation, differentiation, and secondary contact while still maintaining key aspects of a ring model. Hereafter, we refer to such models as "broken" ring models (see Alcaide et al. 2014), with genetic, phenotypic, and/or distributional discontinuities ("gaps") to various degrees.

Monahan et al. (2012) examined the spatial features of ringlike barriers worldwide and predicted that additional examples of ring dynamics might occur around the California Central Valley. This valley, now essentially completely converted to agricultural production, historically included marine seaways and subsequent freshwater lakes (Dupre 1990; Hall 2002), both of which formed barriers to terrestrial taxa. When emergent, the Central Valley acts as a relatively xeric, topography-free lowland barrier to topography-dependent upland taxa. A classic, but debated, example of broken ring speciation exists in *Ensatina* salamanders, where the valley acts as a barrier to upland salamander populations (Stebbins 1949; Moritz et al. 1992; Kuchta et al. 2009; Pereira et al. 2011; Kuchta and Wake 2016).

Here we explore ring speciation in the California endemic spider genus *Calisoga* Chamberlin, 1937. *Calisoga* is a mygalomorph, a clade that includes sedentary taxa such as tarantulas, trapdoor spiders, and relatives (reviewed in Bond et al. 2006; Harvey et al. 2015; Rix et al. 2017). *Calisoga* are relatively large spiders (adult female carapace lengths range from 0.5 to 1.5 cm) that live in subterranean burrows with simple open entrances. According to morphological study, Bentzien (1976) hypothesized that there are only two species of *Calisoga*, including a common, widespread *C. longitarsis* and the smaller, rare *C. theveneti*. Bentzien (1976) hinted that *C. theveneti* are potentially early-maturing *C. longitarsis*, and many arachnologists refer to all Californian nemesiids as *C. longitarsis* (e.g., Ubick and Ledford 2005). A multigenic phylogenetic study confirmed conservative phenotypic evolution in *Calisoga* (particularly in male secondary sexual characteristics) but revealed high levels of genetic divergence, suggesting cryptic speciation with a distribution that mostly encircles the Central Valley (Leavitt et al. 2015).

The population genomic and phylogeographic history of *Calisoga* was examined to test a broken ring model. We tested the following key predictions (see also Irwin and Wake 2016; Kuchta and Wake 2016), with parallels to predictions for an idealized model but allowing for genetic, phenotypic, and/or distributional breaks in a known low-dispersal system: (1) evidence for a single common ancestor for populations involved in the ring complex; (2) a ringlike biogeography, with directionality inferred by phylogenomic patterns and formal biogeographic reconstruction (e.g., Kuchta et al. 2009; Cacho and Baum 2012); (3) diversification timing consistent with known California geology (e.g., populations not older than available landscapes); (4) evidence for gene flow at some point in the evolutionary history of populations, including evidence for isolation by distance (IBD), but allowing for population structuring to various degrees; and (5) evidence for a lack of gene flow and/or phenotypic differentiation at a ring terminus. We stress additional key attributes of a broken ring model in "Discussion" (e.g., persistence on the landscape, slowly evolving reproductive isolation), but we did not explicitly measure or test these variables here. Overall, we find strong evidence for all five tested predictions in *Calisoga*. We highlight the many parallels between *Caligosa* and *Ensatina*, hypothesize other California examples, and discuss more generally how a broken ring model contributes to speciation process knowledge.

Methods

Specimen Sampling

Calisoga were sampled from across their known distribution, including 149 spiders from 115 localities previously collected by Leavitt et al. (2015). To fill minor sampling gaps, we collected 32 spiders from 18 additional localities (table S1; tables S1–S4 are available online). We also sampled 28 individuals from nine localities from near the hypothesized ring terminus, including a location with lineage sympatry. Phylogenomic analyses using out-groups included Mediterranean nemesiid genera *Amblyocarenum* and *Nemesia*, recovered as sister to *Calisoga* in Opatova et al. (2020); one analysis also included more distant mygalomorph genera. Voucher specimens are deposited in the San Diego State University Terrestrial Arthropods Collection (SDSU TAC) and/or the University of California, Davis, Bohart Museum of Entomology (BME).

For most methods summarized below, we provide a brief overview, referring the reader to the supplemental PDF for further details. Analyses and scripts can be accessed in the Dryad Digital Repository (https://doi.org/10.5061/dryad.70rxwdc47; Monjaraz-Ruedas et al. 2024). Data processing was performed on the Mesxuuyan high-performance computing cluster at SDSU.

UCEs, Mitochondrial Data, Nuclear SNPs

Nuclear ultraconserved element (UCE) data were processed using a pipeline that included software packages Trimmomatic (Bolger et al. 2014), SPAdes (Prjibelski et al. 2020), PHYLUCE (Faircloth 2016), MAFFT (Katoh et al. 2009), Gblocks (Castresana 2000), CIAlign (Tumescheit et al. 2022), and FUSe (https://github.com/rmonjaraz/FUSe). Raw

UCE data are deposited under BioProject PRJNA1073270 in the GenBank Sequence Read Archive repository.

Mitochondrial protein coding loci were captured as UCE bycatch using custom scripts (mtdna_byCatch.sh, Dryad Digital Repository [https://doi.org/10.5061/dryad.70rxwdc47; Monjaraz-Ruedas et al. 2024]) and methods detailed in the supplemental PDF. A concatenated mitochondrial matrix including out-group nemesiid genera was analyzed using maximum likelihood (ML) with IQ-TREE 2 (Minh et al. 2020*b*). Selection of the best partition (loci as different partitions) and fitting of the best substitution model were performed with ModelFinder using the Bayesian information criterion (Kalyaanamoorthy et al. 2017), with branch support assessed with 1,000 replicates of ultrafast bootstrap (Hoang et al. 2018).

We extracted single-nucleotide polymorphism (SNP) data from UCE alignments following Zarza et al. (2018) and the PHYLUCE (ver. 1.7.1) mapping workflow (snps_calling.sh, Dryad Digital Repository [https://doi.org/10.5061/dryad.70rxwdc47; Monjaraz-Ruedas et al. 2024]). We used UCE final alignments after the "per sample" filtering process as a pseudoreference, minimizing possible paralogs and/or sequencing errors. SNP variants were called using BWA (Li 2013) and BCFtools (ver. 1.11; Danecek et al. 2021) and filtered using VCFtools (ver. 0.1.16; Danecek et al. 2011; see also the supplemental PDF). Using a custom perl script (randSnps.pl, Dryad Digital Repository [https://doi.org/10.5061/dryad.70rxwdc47; Monjaraz-Ruedas et al. 2024]), the resulting VCF file was subsampled retaining one random SNP per locus (retrieving unlinked SNPs).

Prediction 1: Ring Complex Common Ancestry

Phylogenomic and biogeographic analyses were conducted to confirm a monophyletic ring complex, with populations surrounding a central barrier. Multiple UCE matrices were created for these analyses (table S2). An 80% occupancy out-group matrix included two more samples (183 samples, 1,244 UCEs) than a matrix including only *Calisoga* specimens (in-group matrix: 181 samples, 1,246 UCEs). Smaller in-group matrices were created corresponding to recovered North and South clades, subsampling loci with the highest ratio of parsimony-informative sites (North matrix: 200 UCEs, 73 samples; South matrix: 200 UCEs, 93 samples).

ML analyses as above were conducted using the out-group and in-group matrices. Variation in ML tree topologies was assessed using gene and site concordance factors (Minh et al. 2020*a*; Lanfear and Hahn 2024). A species tree was estimated under a quartet summary method using ASTRAL (ver. 5.7.7; Mirarab and Warnow 2015; Zhang et al. 2018; Rabiee et al. 2019) with both out-group and in-group matrices. Input ASTRAL gene trees were estimated using ML as described above and treated as unrooted. Internal branch lengths were estimated in coalescent units, with branch support measured as local posterior probability values (Sayyari and Mirarab 2016); topological variation was assessed using quartet scores (Lanfear and Hahn 2024).

Predictions 2 and 3: Divergence Time Estimation and Biogeographic Reconstruction

To test for diversification timing consistent with California landscape availability, particularly South Coast Range habitat availability, we calculated divergence times using a multispecies coalescent model implemented in the BEAST2 package SNAPPER (Stoltz et al. 2021). We subsampled the out-group matrix to 70 specimens (representing all primary phylogeographic lineages; see "Results") and called SNPs without missing data, resulting in 413 unlinked biallelic SNPs. To convert coalescent units into time-calibrated branch lengths, we followed Stange et al. (2018), using secondary calibrations from Opatova et al. (2020). Input files were generated using the script snapp_prep.rb (https://github.com/ForBioPhylogenomics/tutorials/tree/main/divergence_time_estimation_with_snp_data). We set all 70 individuals as separate species, using ASTRAL trees as a starting point (flag -s). Absolute time calibration details are provided in the supplemental PDF.

Analyses of biogeographic directionality and ancestral range estimation were conducted using the dispersal-extinction-cladogenesis (DEC) model (Ree and Smith 2008), implemented in BioGeoBEARS (Matzke 2014). The SNAPPER maximum clade credibility tree was used as input, collapsed to represent primary phylogeographic lineages as terminal taxa. Geographic ranges as states were scored in a presence/absence matrix following well-recognized phytogeographic subdivisions for California (Burge et al. 2016; Baldwin et al. 2017). Analyses were run with default parameters setting the range number to four, maximum range number to two, and maximum range size to two, without dispersal or time constraints.

Prediction 4: Population Structure and Nuclear Gene Flow

Population units for population structure and gene flow analyses were inferred using tree-based (phylogenomic) and SNP-clustering approaches. For the tree-based approach, we defined "primary phylogeographic lineages" as geographically cohesive clades recovered consistently across nuclear analyses, with high support or topological concordance measured in multiple ways (bootstrap, posterior probability, site concordance factors). We are unaware of a consensus definition for "phylogeographic lineage." Our phylogeographic

lineages are more subdivided than "populations," as inferred from cluster analyses (see below), but less subdivided than other possible phylogenetic definitions. We used the Bayesian phylogenetics and phylogeography program (BPP; Yang and Rannala 2010, 2014; Flouri et al. 2020) to validate phylogeographic lineages, following the argument that multispecies coalescent methods are efficient at delineating Wright-Fisher populations (Sukumaran and Knowles 2017).

Algorithmic genetic clustering was implemented using sparse nonnegative matrix factorization (sNMF) in the R package LEA (Frichot et al. 2014; Frichot and François 2015), using the unlinked SNPs dataset. Ten runs with 1×10^5 iterations and $\alpha = 10$ were performed for K values ranging from 1 to 15; a cross-entropy validation method was used to select an optimal K value. We also assessed genetic clustering using TESS3 (Caye et al. 2016), which estimates genetic ancestry coefficients taking geography into consideration. Input data included unlinked SNPs for K 1–20 groups using a projected.ls method with 10 replicates and 10,000 iterations, using the R package tess3r (Caye et al. 2016).

A ring species model predicts IBD at nonterminal parts of the ring (Irwin et al. 2001; Irwin and Wake 2016; Kuchta and Wake 2016). We tested for IBD using individual pairwise Euclidean genetic (from all SNPs) and geographic distances, assessing significance with a Mantel test with 1,000 bootstrap replicates. Analyses were conducted in the R packages adegenet and dartR (Jombart 2008; Jombart and Ahmed 2011; Gruber et al. 2018). We grouped individuals into primary phylogeographic lineages, sNMF genetic clusters at optimal K values, and broader North versus South clades. Because the latter analysis involved geographic distance comparisons across the Central Valley, we created a custom conductance raster to penalize straight-line distances directly spanning the valley (see the supplemental PDF).

The F_{ST} values were calculated among primary phylogeographic lineages using dartR; data were imported into a genlight object using the package vcfR (Knaus and Grünwald 2017). Gene flow between primary phylogeographic lineages was measured using ABBA-BABA tests (Patterson et al. 2012; Malinsky et al. 2021), implemented in Dsuite (Malinsky et al. 2021). We computed all combinations of trios using the full SNP dataset, assigning the Sacramento lineage as the out-group (see "Results"). The P values were adjusted using the p.adjust function in R using the Benjamini-Hochberg correction (Benjamini and Hochberg 1995). The F_4-ratio and F-branch plots were plotted using Dsuite accompanying scripts, using the ASTRAL topology as a reference tree.

FEEMS (ver. 1.0; Marcus et al. 2021) was used to identify geographic regions with gene flow restriction. FEEMS estimates migration parameters using a penalized-likelihood framework, using a fast quasi-Newton optimization algorithm (Marcus et al. 2021). We used the full SNP dataset, converted from vcf to bed format using plink2 (Chang et al. 2015). In this method, λ is a tuning parameter used to penalize the strength of migration; we selected the λ that minimized cross-validation error by running 20 values of λ from $1e^{-6}$ to $1e^{-2}$.

Prediction 5: Contact at Ring Terminus

To test for a lack of gene flow at the ring terminus, we assembled a contact zone matrix (1,119 UCEs, 12 Bay and 16 South samples) including 15 additional specimens from a syntopy location (Coalinga Road) first reported by Leavitt et al. (2015). Geographically adjacent Bay and South specimens were included for broader geographic context (table S1). We conducted ML analyses as above and also extracted unlinked SNPs and used sNMF with K ranging from 1 to 6.

Morphological differentiation at the ring terminus was examined by measuring adult female voucher specimens available for the contact zone matrix ($n = 10$). A series of linear measurements for 12 continuous variables was taken (table S3). To place morphological differentiation at ring contact into a broader context, we also took measurements of adult female voucher specimens for the entire in-group matrix ($n = 159$). A multidimensional scaling (MDS) analysis was performed using the R package stats, function dist() and cmdscale(), computing Euclidean distances and decomposing the data to a maximum of two dimensions ($k = 2$). We also conducted a principal components analysis (PCA) using the R package FactoMineR (Lê et al, 2008) and used PC1 scores to calculate average pairwise Euclidean distances between specimens grouped by primary phylogeographic lineage. Finally, we used PC1 Euclidean distances to examine the relationship between morphological and geographic individual pairwise distances for groupings of North and South clades, excluding syntopy specimens. Significance was assessed using a Mantel test with 1,000 bootstrap replicates.

Results

Data

Input, log, and output files are available in the Dryad Digital Repository (https://doi.org/10.5061/dryad.70rxwdc47; Monjaraz-Ruedas et al. 2024). We recovered an average of 1,345 UCEs per sample with a mean length of 950 bp without filtering or trimming. The in-group matrix included 1,246 UCEs and a concatenated length of about 800 kbp. The filtered VCF file included 5,941 biallelic SNPs for 176 samples, including 983 unlinked SNPs. We recovered

15 mitochondrial genes for 192 samples, including 9 samples not included in nuclear analyses (table S4). Matrix details are found in table S2.

Prediction 1: Ring Complex Common Ancestry

Nuclear phylogenomic analyses agreed in recovering a monophyletic *Calisoga*, with well-supported Sacramento, North, and South subclades (figs. 1*A*, S1–S3, S6; figs. S1–S13 are available online). Analyses including nemesiid out-groups place a Sacramento lineage as sister to a monophyletic ring complex (North + South) in three of four analyses (concatenated, SNAPPER, mitogenomic). In the ASTRAL outgroup analysis, Sacramento is placed inside the ring complex, sister to North, but with low support (0.85 posterior probability; fig. S1). An ASTRAL analysis with a larger sampling of mygalomorph taxa recovers Sacramento as sister to a monophyletic ring complex with strong support (fig. S2). We hereafter treat the Sacramento lineage as a closely related sister species to the ring complex and exclude

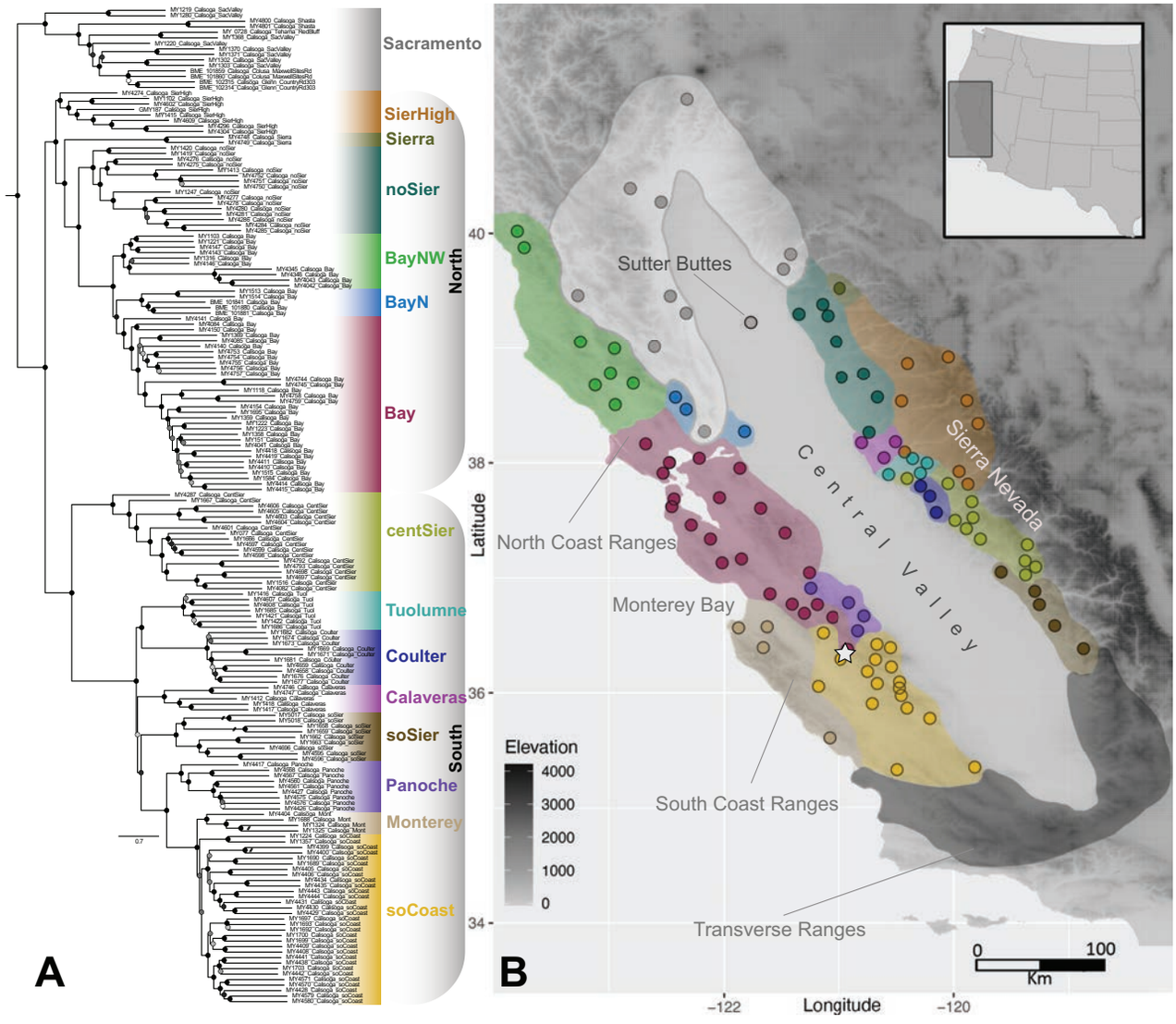

Figure 1: *Calisoga* phylogeographic structure. *A*, ASTRAL tree showing relationships of primary phylogenomic lineages. Node circles denote local posterior probability support, colored in grayscale with values >0.95 in black and values <0.5 in white. *B*, Distribution of *Calisoga* samples, with colors matching primary phylogenomic lineages. Highlighted are major geographic features discussed, including the Sierra Nevada mountains, North and South Coast Ranges, Transverse Ranges, Sutter Buttes, and Monterey Bay. We note that *Calisoga* has never been recorded from the Transverse Ranges. A star designates the sampled sympatry location.

Sacramento samples from population genomic analyses focused on ring speciation dynamics.

Six and eight primary phylogeographic lineages were recovered within North and South clades of the ring complex, respectively (fig. 1; table S1). Primary phylogeographic lineages were validated with BPP, all recovered with a posterior probability of 1. Phylogeographic lineages and lineage interrelationships are generally well supported using bootstrap and posterior probabilities (figs. 1*A*, S1, S3); relevant branches also show less topological variation, as assessed by quartet scores and site concordance factors (figs. 1*A*, S1, S3). Mitogenomic analyses with nemesiid out-groups recover a Sacramento lineage sister to a monophyletic ring complex, and within North and South clades, relationships are broadly similar (but not identical) to those found in nuclear analyses (fig. S4).

North and South clades have approximately parallel internal phylogenomic structuring, with a high-elevation clade in the west-central Sierra Nevada sister to remaining lineages, which themselves show well-supported east-to-west paraphyly (figs. 1, S1, S3, S4). In the North this includes spider populations in the northern Sierra Nevada foothills, with derived populations in the North Coast Ranges, including the Bay Area. The South clade includes spiders in the central and southern Sierra Nevada foothills, with derived populations in the South Coast Ranges (figs. 1, S1, S3, S4). Along Coalinga Road in the South Coast Ranges, northern spiders are sympatric with southern spiders near the ring terminus (see below).

Predictions 2 and 3: Divergence Time Estimation and Biogeographic Reconstruction

Analyses based on nuclear SNPs estimate a divergence of *Calisoga* from other nemesiid genera around 83 million years (myr) ago (78.8–86.7 95% highest posterior density [HPD]), with a most recent common ancestor (MRCA) of Sacramento plus the ring complex in the Late Miocene (7.5–12.7 95% HPD; figs. 2, S6). Divergence of the MRCA of the ring complex is estimated at 9 myr ago, with the MRCA of individual North and South clades estimated at 7 and 8 myr ago, respectively (figs. 2, S6). Importantly for the ring species hypothesis, western South clade members share an estimated common ancestor 4.5 myr ago, when emergent terrestrial habitats would have been available in this geographic region (Hall 2002). Upland habitats in the Sierra Nevada and North Coast Ranges were also available from 5 to 7 myr ago (Harden 1998; Furlong and Schwartz 2004; Schierenbeck 2014).

DEC analyses indicate the Sierra Nevada region as the most probable ancestral range for the MRCA of the ring complex, with a ML probability >75% for Sierra Nevada and a lower probability for the northwestern and Sierra Nevada regions (NW + SN in fig. 2). In both North and South clades, ancestral range reconstructions transition from the Sierra Nevada to Coast Ranges, in both the north (northwestern and central western regions; NW + CW) and the south (CW).

Prediction 4: Population Structure and Nuclear Gene Flow

Genetic population clusters are consistent with, but generally more conservative than, primary phylogeographic lineages (figs. 3, S7). The value $K = 5$ corresponds to the best cross-validation value (fig. 3*B*, 3*C*), but we also show $K = 14$ to compare directly with recovered phylogeographic lineages. Multiple possible admixed specimens were observed at $K = 5$, principally in Sierra and Calaveras lineages. This possible admixture mostly disappears when increasing K to 14 (fig. 3*B*, *bottom*). Monterey was recovered as part of the same genetic cluster as SoCoast, even when increasing K values. TESS3 analyses agree with sNMF in finding five clusters when considering landscape context, with the same subdivision into North and South clades (fig. 4*A*). This clustering scheme is again conservative with respect to primary phylogeographic lineages.

Analysis of IBD with individual samples grouped into North and South clades, $K = 5$ sNMF clusters, and primary phylogeographic lineages revealed a significant positive result for all (figs. 3*D*, 3*E*, S8). Significant results are also found for North and South geographic distance comparisons corrected for distances across the Central Valley (fig. 3*D*). However, these significant results at all levels of clustering conceal important differences among IBD analyses. In particular, as groupings become more inclusive, IBD slopes in general become less steep (figs. 3*D*, 3*E*, S8).

The F_{ST} values indicate high population differentiation among primary phylogeographic lineages, ranging from 0.37 to 0.83 (fig. 4*B*). A pattern of increasing pairwise values with increasing geographic distance is observed in the North clade (e.g., SierHigh vs. other populations; fig. 4*B*), but this stepwise pattern is not observed in the South clade. Instead, F_{ST} values are consistently high in the South clade, both across lineages in the Sierra Nevada and for comparisons across the Central Valley (fig. 4*B*).

ABBA-BABA results indicate limited gene flow among primary phylogeographic lineages (fig. 4*D*). Although these tests cannot measure gene flow between sister lineages, given the *Calisoga* tree structure, this pertains only to three sister lineage comparisons; most tested comparisons are across nonsisters, even when lineages are geographically adjacent. Evidence for gene flow within the South clade is present in lineages of the Sierra Nevada. Evidence for gene flow within the North clade is found between adjacent high-elevation (SierHigh) and low-elevation (noSier)

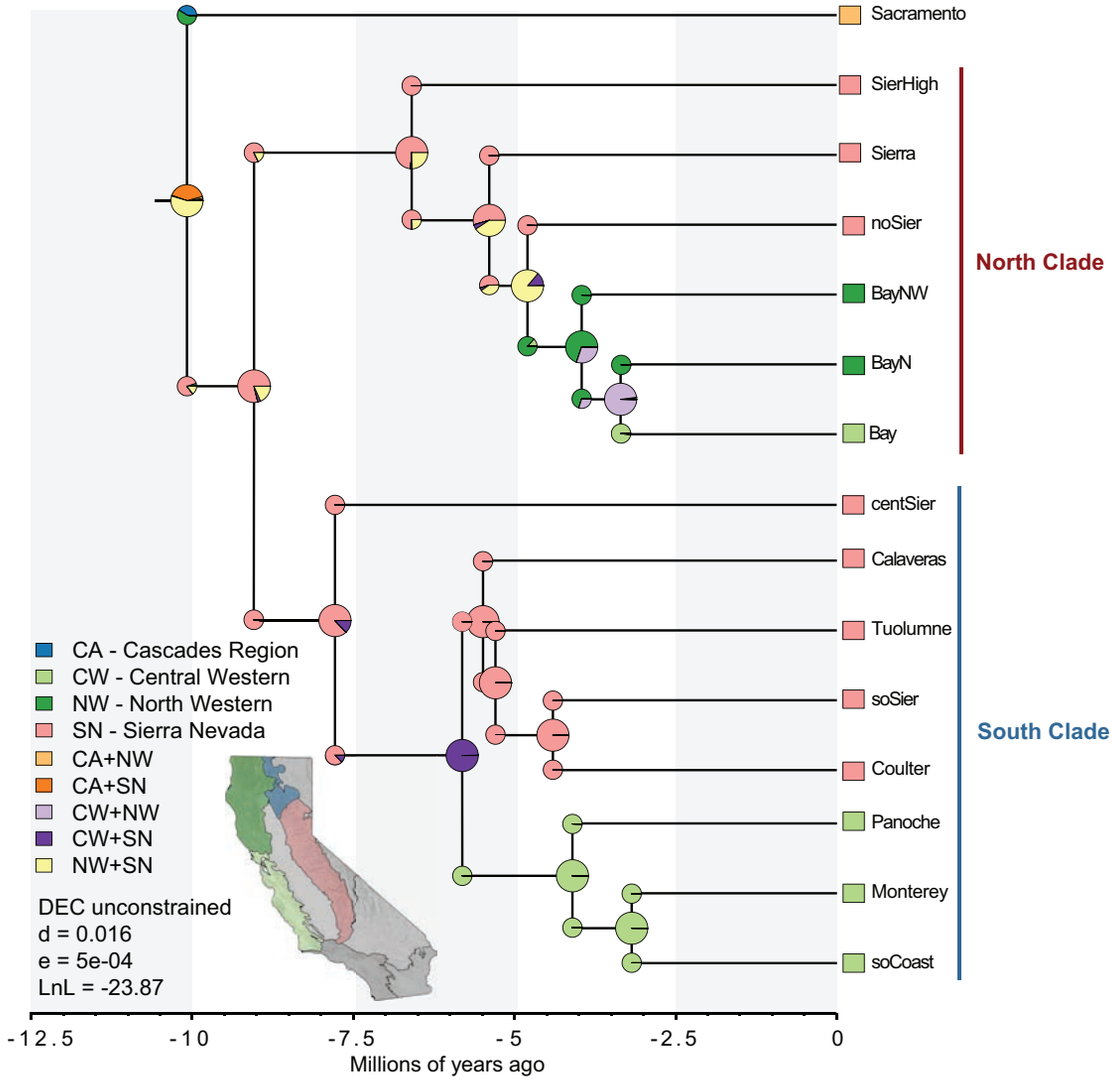

Figure 2: *Calisoga* ancestral range estimation under a dispersal-extinction-cladogenesis (DEC) model. Pie charts show ancestral range reconstruction probabilities for each node; distribution ranges for each phylogeographic lineage are represented by squares at the tips. Time axis is in millions of years.

lineages. Gene flow was also detected between the North and South clades (fig. 4*D*). Here, patterns of gene flow from one population repeated in multiple different populations are interpreted as ancestral gene flow (Malinsky et al. 2021), in this case between SierHigh and noSier in the North clade with the ancestor of the South clade. The *F*-branch results (fig. S9) are congruent with the above but slightly more conservative (less significant).

FEEMS analysis at best-fit $\lambda = 100$ shows high gene flow resistance across the Central Valley and at terminal contact (fig. 4*C*). Different values of λ revealed areas with high gene flow resistance in agreement with phylogeographic lineages within North and South clades and further suggest that gene flow is more restricted in the ancestral ranges of the Sierra Nevada and less restricted in western locations, except at the ring terminus (e.g., $\lambda = 0.8$ or $\lambda = 14$; fig. S10).

Prediction 5: Contact at Ring Terminus

Phylogenomic analysis of a subsample of Bay and South specimens from in and near the syntopy site along Coalinga Road (contact zone matrix) resulted in reciprocally monophyletic groups (fig. 5*A*), with $k = 2$ sNMF clusters (fig. S11). Bay and South spiders from the syntopy site show no signs of genetic admixture (fig. 5*B*), even when

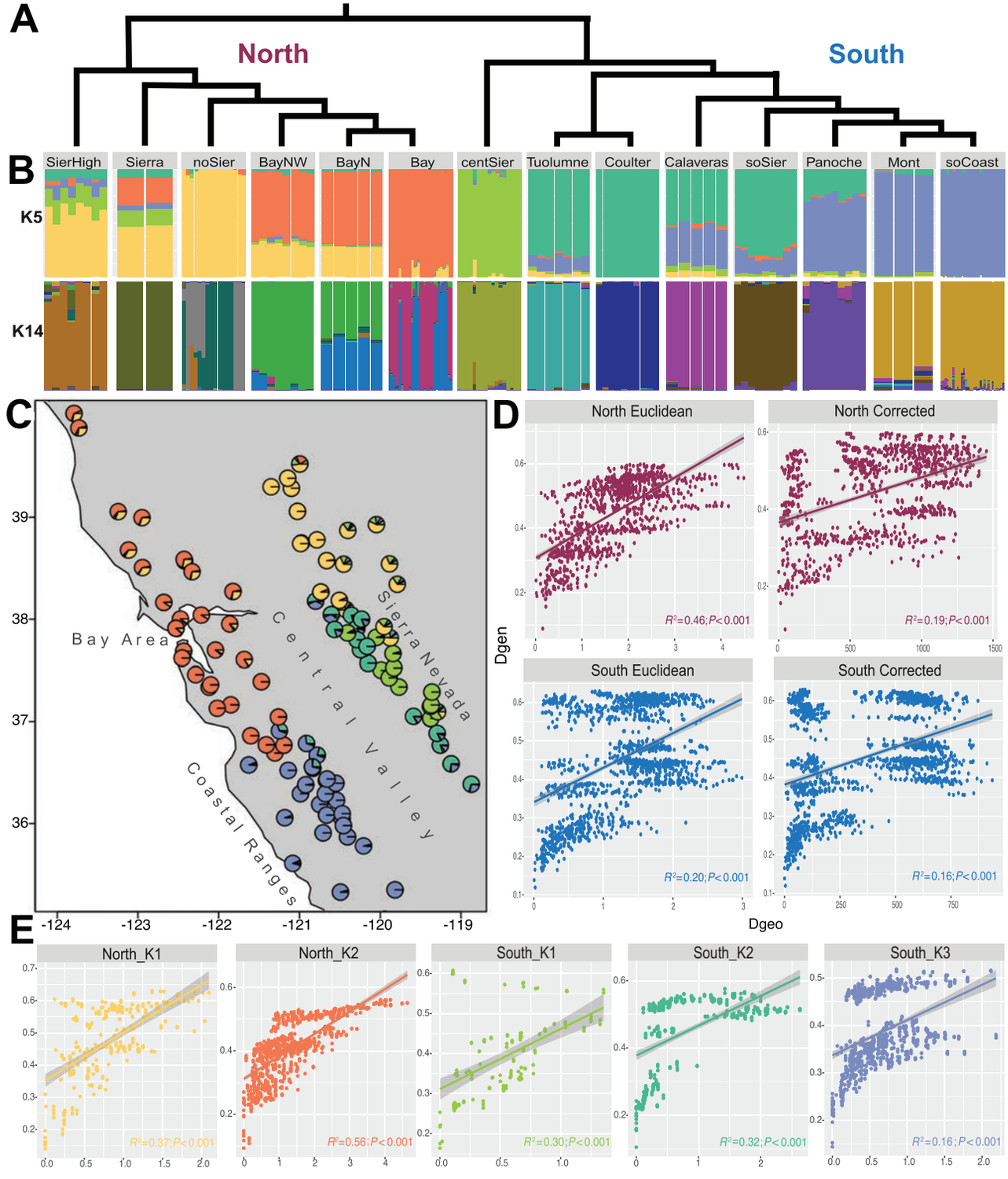

Figure 3: *Calisoga* population structure. *A*, ASTRAL tree with major phylogeographic lineages. *B*, Sparse nonnegative matrix factorization (sNMF) ancestry coefficients with *K* values of 5 (optimal) and 14. *C*, Map of $K = 5$ sNMF ancestry proportions. *D*, *E*, Isolation-by-distance results for individual pairwise values grouped into North and South clades (*D*) and $K = 5$ sNMF clusters (*E*).

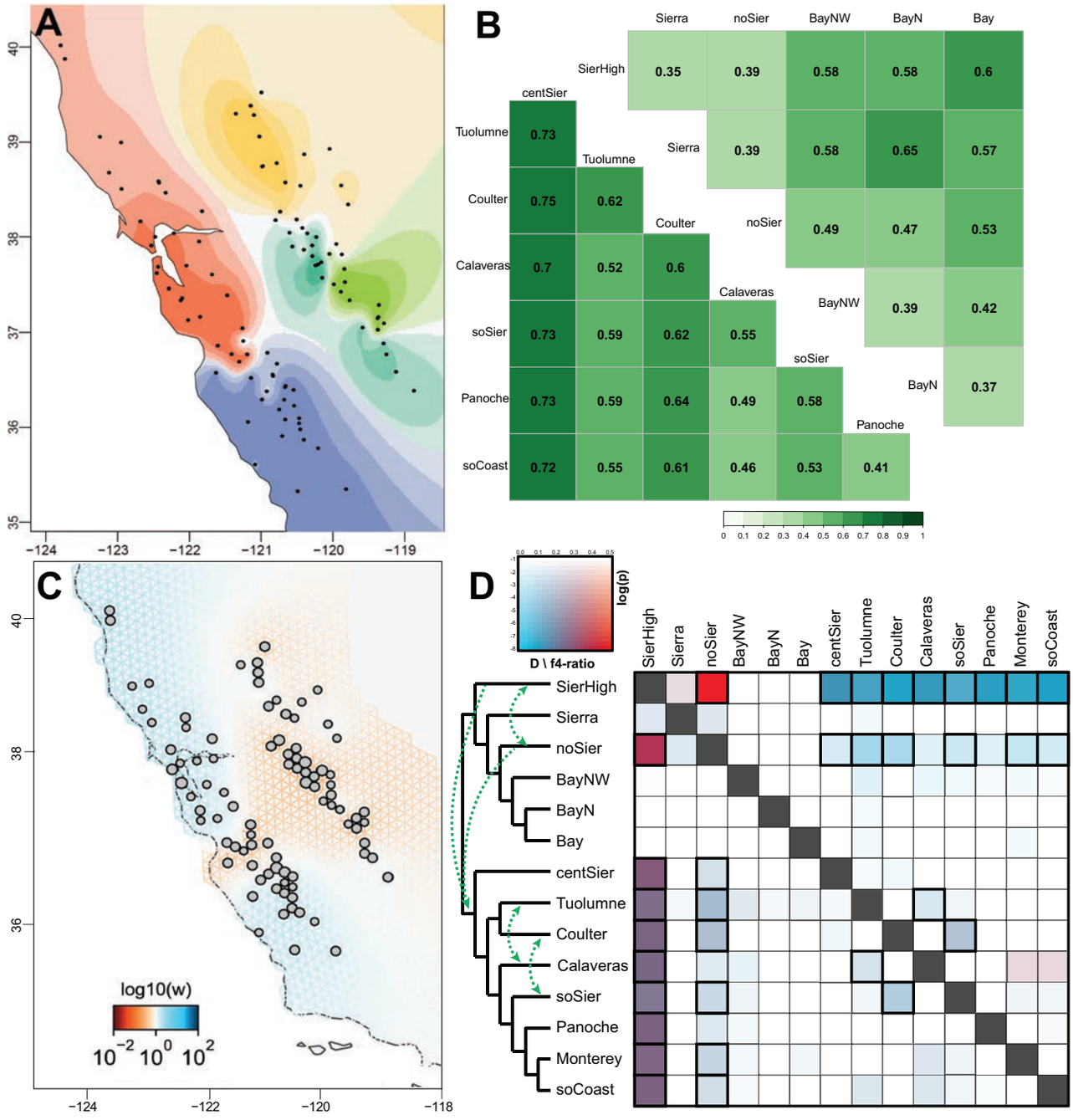

Figure 4: *Calisoga* population structure and gene flow. *A*, TESS3 $K = 5$ ancestry coefficients. *B*, Pairwise F_{ST} values for phylogeographic lineages within North and South clades. *C*, FEEMS-estimated migration surfaces, $\lambda = 100$. Gray circles denote sample assignments in the grid, and size denotes number of samples assigned to that specific node. Cooler colors (in blue) correspond to higher than average gene flow through time, while warmer colors (in brown) correspond to lower than average gene flow through time. *D*, Heat map showing admixture proportions and *P* values of ABBA-BABA tests between phylogeographic lineages. Values below the diagonal correspond to *D* statistics results, and values above the diagonal correspond to the F_4 ratio. Cells with thicker margins correspond to significant results after *P* value correction. Green arrows in the left-hand tree denote significant gene flow detected between phylogeographic lineages.

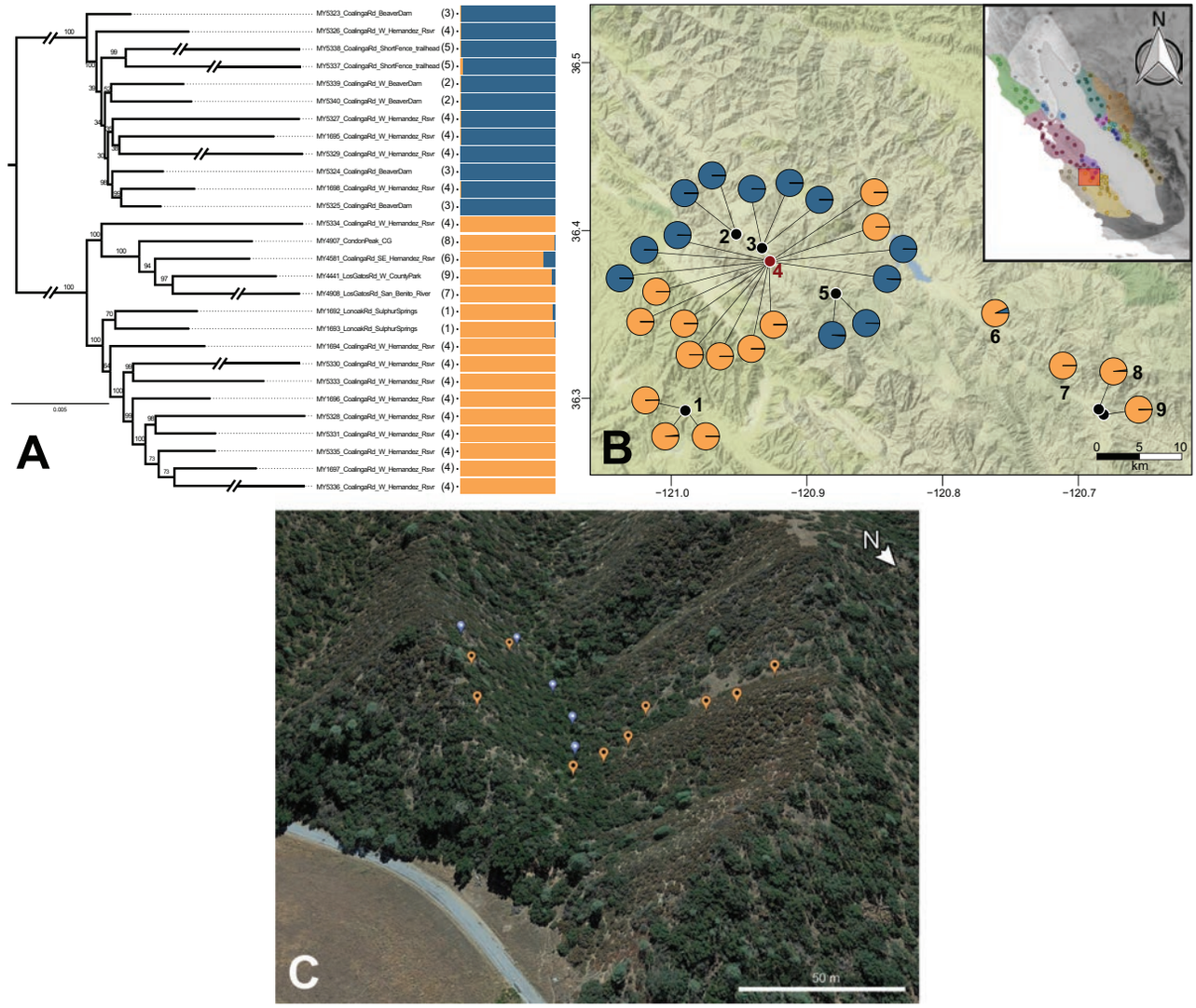

Figure 5: Terminal contact patterns in *Calisoga*. *A*, Maximum likelihood phylogeny showing relationships for the contact zone matrix. Branch labels indicate bootstrap support values, with some branches trimmed for visual purposes. Shown to the right of the tree are sparse nonnegative matrix factorization (sNMF) ancestry coefficients at $K = 2$. Location numbers (in parentheses) to the left of ancestry coefficients match locations shown in *B*. *B*, Detailed map of the South Coast Ranges showing sampling locations and their respective sNMF ancestry coefficients. Location 4 corresponds to the original sympatry location (MCH 09_042, along Coalinga Road, west of Hernandez Reservoir). *C*, Microgeographic distribution of specimens at the sympatry location. Darker greens (north facing) are dominated by oak trees, and lighter browns (south facing) are dominated by chamise.

collected from burrows only 10 m apart (fig. 5*C*). Possible admixture was observed for a single spider not from the syntopy site (MY4581; fig. 5), but this might be an artifact of this sample being more related to unsampled eastern individuals (fig. 3*B*).

MDS analysis recovered high morphological similarity among *Calisoga* samples (goodness of fit = 0.93), with phylogeographic lineages and major clades (North, South) overlapping in Euclidean distance space (fig. 6*A*). PC-derived morphological distances between major clades generally exceed those within clades (fig. 6*C*). Morphological IBD is nonsignificant in both North and South clades (fig. S13).

Samples from Bay and SoCoast lineages in syntopy at Coalinga Road show pronounced morphological differentiation (fig. 6*B*). Average pairwise Euclidean distances from PC1 scores were 3.03, 2.97, and 5.35 between members of North versus South clades, Bay versus SoCoast lineages

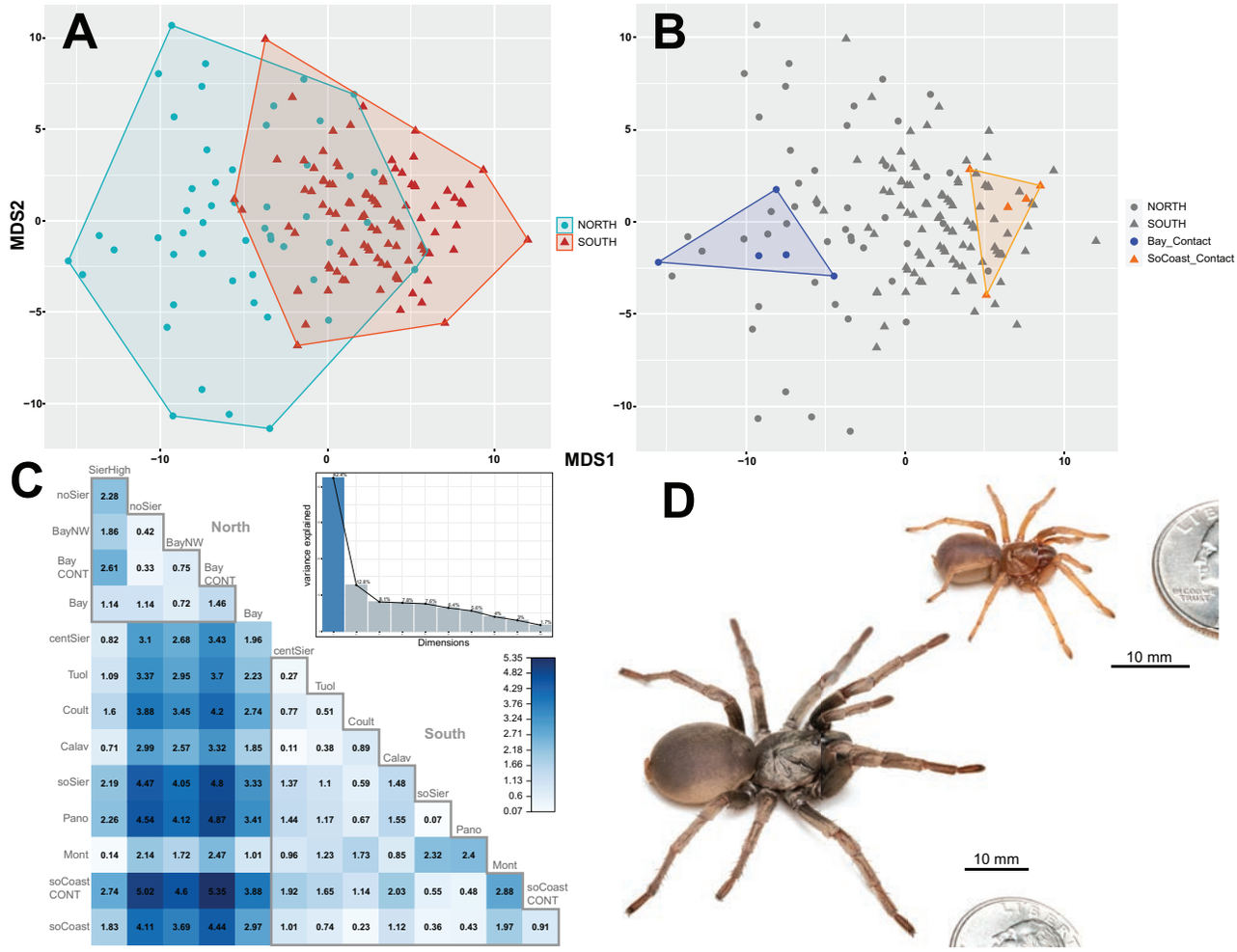

Figure 6: *A*, *B*, Multidimensional scaling analysis of 12 morphological variables (table S3) for North and South clades only (*A*) and North and South clades, highlighting samples from Bay and SoCoast phylogeographic lineages found at Coalinga Road (*B*). *C*, Pairwise Euclidean distances among phylogeographic lineages, calculated from principal component 1 scores (see inset). BayN samples were not available for this analysis. *D*, Example of phenotypic variation observed at the Coalinga Road location (small blonde spider is from SoCoast, large dark spider is from Bay).

(excluding syntopy site specimens), and syntopy site specimens, respectively (fig. 6*C*). On average, the morphological distance between specimens in the contact zone is higher than average values across phylogeographic lineages or larger clades; these distances in fact exceed all other pairwise distances in the ring complex (fig. 6*C*). In syntopy there is no overlap between specimens in carapace length or in cheliceral microteeth (table S3). Although microhabitat was not formally quantified, small-bodied SoCoast spiders occupied burrows on more open ground near or under chamise, while large-bodied Bay spiders preferred shaded oak woodland with thicker leaf litter (figs. 5*C*, 6*D*; M. Hedin, personal observation). This microhabitat partitioning was essentially perfect at the syntopy site, in a heterogeneous habitat including adjacent north-facing (oak-dominated) and south-facing (chamise-dominated) plant communities (fig. 5*C*).

Discussion

Idealized ring species remain to be discovered or perhaps do not exist in nature (Joseph et al. 2008; Monahan et al. 2012; Alcaide et al. 2014; Wang et al. 2021), prompting Kuchta and Wake (2016) and Irwin and Wake (2016) to summarize more realistic empirical conditions and examples of broken ring species. We similarly contend

that a broken ring model should be the default, retaining key aspects while being closer to empirical reality. Below, we return to the five predictions set forth in the introduction, highlighting strong evidence for all in *Calisoga*.

Common Ancestry, Ringlike Biogeography, and Timing

The slopes of the Sierra Nevada are reconstructed as the ancestral area for the ring complex, with parallel phylogenomic and distributional arms extending from east to west around the Central Valley (figs. 1, 2) and timing consistent with landscape availability. Estimated diversification times for lower-elevation lineages within both North and South clades also approximately correspond to the onset of a Mediterranean climate in California around 5 myr ago (Ackerly 2009; Lancaster and Kay 2013).

Our data support the Sacramento lineage (fig. 1*B*) as sister to the *Calisoga* ring complex. Although the Sacramento lineage occupies the northern Central Valley and appears to naturally form the northern part of a ring distribution (fig. 1*B*), we instead hypothesize a "truncated" northern transvalley distribution for the ring complex. It remains possible that ecological interactions with the Sacramento lineage have impacted the northern distribution of the ring complex, but these populations lie evolutionarily outside of the ring complex proper.

Although almost all of the *Calisoga* records are from upland habitats (to various degrees), these spiders can infrequently occupy low-elevation valley habitats, as shown by Bay lineage Jepson Prairie collections (at 2–8 m asl). Although we (and others) have framed the valley as a "long-term barrier," woodland or chaparral habitats have constricted the valley latitudinally at both northern and southern ends multiple times in the past, including during the late Miocene to Pliocene (Axelrod 1973), providing possible dispersal opportunities for *Calisoga*. As such, a contiguous ring may have existed for the *Calisoga* ring complex but has since evaporated as dispersal corridors have retracted. In the north we hypothesize a latitudinal crossing near the current Sutter Buttes (fig. 1*B*). In the south a late Miocene to Pliocene San Joaquin Basin marine embayment (Bowersox 2005, fig. 8) extended to the Transverse Ranges. We hypothesize that southern transvalley dispersal was actually north of this barrier, at a latitude consistent with the western Panoche lineage (fig. 1*B*). It also remains possible that the southern distributional gap is an artifact and that *Calisoga* are found in the southern Transverse Ranges (fig. 1*B*), although we have never encountered them here in our more than two decades of California mygalomorph collecting. Overall, the broken *Calisoga* ring is hypothesized to be truncated in comparison to the full latitudinal extent of the modern Central Valley.

Contrasting Pictures of Population Connectivity

Calisoga populations are genetically structured by geography, and this genetic structuring is hierarchically organized. TESS3 and sNMF at optimal K suggest relatively few genetic units (five), and these units appear to be connected by higher amounts of gene flow (e.g., figs. 3*B*, 3*C*, 4*A*). Importantly, at these optimal K values, admixture among geographically adjacent populations is gradual and approximately continuous. Also, either sNMF clusters or more inclusive North and South clades as population units show evidence for positive and significant IBD (fig. 3*D*, 3*E*). Together, these multiple analyses are more consistent with connectivity expectations of an idealized ring model, with relatively few units connected by higher amounts of genetic exchange over broader geographic regions.

Simultaneously, there are hierarchically nested phylogeographic lineages found within these broader genetic groupings, as revealed by phylogenomic and sNMF at $K = 14$ analyses (figs. 1, 3*B*). We conservatively defined primary phylogeographic lineages with contiguous geographic distributions, which are consistent across nuclear analyses, and recovered with high support for various metrics. Because our spatial sampling is fine-grained and extensive, amassed over a decade of fieldwork, we contend that phylogenetic distinctions among primary phylogeographic lineages are not an artifact of gappy sampling (Mason et al. 2020). These lineages are genetically divergent, as shown by F_{ST}, and when increasing the number of sNMF clusters to $K = 14$, signs of individual admixture disappear (fig. 3*B*). Overall, these analyses would paint a picture of less population connectivity, contra above.

Nested IBD analyses also reveal hierarchical population structuring. Although IBD slopes are significantly positive at all levels of nesting, slopes vary across analyses and become less steep with more inclusive groupings (figs. 3*D*, 3*E*, S8). We hypothesize that this results from the lumping of genetically divergent subpopulations, easily visualized in several inclusive IBD plots that show distinct clouds of points. These distinct clouds comprise the distance comparisons across individuals in divergent phylogeographic lineages, which show higher genetic distances at comparable geographic distances.

A fundamental issue regarding the conceptualization and measurement of connectivity involves recognizing units of evolution. Are population units defined by best-fit sNMF, TESS3, and FEEMS too conservative? Are primary phylogeographic lineages too fine-grained, reflecting artificial discontinuity in a relatively more continuous system? We argue that both conservative and fine-grained

patterns can exist simultaneously, reflecting fractal and hierarchical structuring, as also found in *Ensatina* (summarized below).

Terminal Contact

The distributions of North and South clades intertwine in the northwest-trending valleys of the Diablo Range, southeast of Monterey (figs. 1, 5), where northern individuals interact with distantly related southern spiders. We consider this Diablo Range geographic region to represent the approximate ring terminus. Focused sampling at Coalinga Road reveals no gene flow, despite intimate geographic proximity of specimens (fig. 5*A*, 5*B*). Specimens from divergent phylogenomic lineages at this location are clearly both morphologically and ecologically distinct, with levels of morphological difference that exceed allopatric parts of the ring (fig. 6).

The sampled Diablo Range syntopy site is likely one of many contact locations in this general region, although no other such locations have been discovered. Discovering close parapatry or syntopy is challenging in these burrowing spiders, requiring microgeographic-scale sampling and many return field visits. The paleogeographic history of the Diablo Range region lends credence to this area as a phylogeographic merging grounds (Kuchta and Tan 2006). From approximately 8 to 2.2 myr ago, a large marine embayment extended from just north of Monterey southeastward, filling most of the southern San Joaquin Valley (Dupre 1990; Hall 2002, plates 6–8; Bowersox 2005, fig. 8; Powell et al. 2007). The transition from marine to freshwater 2.2 myr ago may have allowed Bay and SoCoast spiders to move into contact, consistent with molecular clock analyses (e.g., southern Bay populations MRCA less than 2 myr ago; fig. S6).

Parallels with Ensatina*, Other Possible California Ring Species*

Ensatina salamanders represent one of the most well-cited cases of ring speciation (summarized in Irwin and Wake 2016; Kuchta and Wake 2016), technically broken ring speciation. *Ensatina* are sedentary animals with small home ranges (e.g., Staub et al. 1995). Genetic studies of *Ensatina* have found deep structuring, measured by nuclear allozymes (Wake and Yanev 1986; Jackman and Wake 1994; Wake 1997; Pereira and Wake 2009; Pereira et al. 2011) and mitochondrial divergences (Moritz et al. 1992; Kuchta et al. 2009). Moreover, this genetic structuring has been characterized as "fractal," or hierarchically organized, with smaller units nested within larger units, as argued above for *Calisoga*. Distributional gaps are found in *Ensatina*, where local population extinction is hypothesized to have occurred (Jackman and Wake 1994). Also, as for *Calisoga*, the general spatial concordance between nuclear and mitochondrial lineages suggests that the arrangement of distinct genetic lineages results from historical isolation rather than from stochastic lineage breaks. Overall, in places other than the terminus, *Ensatina* is a system with ubiquitous genetic differentiation without absolute isolation (Pereira and Wake 2009).

Although the Central Valley represents a geographic barrier with long-term (evolutionary) persistence and topographic features expected to promote ring speciation (Monahan et al. 2012), few other documented examples exist. Our detailed knowledge of California arthropods leads us to anticipate additional, currently unexplored, examples in this fauna. Species or species groups with ring-like geographic distributions include California night-stalking tiger beetles (*Omus californicus*; Cazier 1942), *Titiotus* spiders (Platnick and Ubick 2008), certain clades of *Aliatypus* trapdoor spiders (Satler et al. 2013), and *Gosodesmus* millipedes (Buckett and Gardner 1969). All of these taxa would likely correspond to broken ring species, again because these are small-bodied, ground-dwelling, dispersal-limited animals existing in a topographically complex landscape. We discuss other attributes below (e.g., extinction resistance, slowly evolving reproductive isolation) that in combination may promote ring speciation in dispersal-limited animals.

Extending the Broken Ring Model

The empirical reality is that all ring species are expected to be broken to various degrees. Species do not exist on a blank homogeneous geographic canvas. The details and complexities of landscape history are not nuisance parameters but rather are interesting to study in their own right. Broken ring species provide such detailed biogeographic insight. But what else can we learn about speciation from broken ring systems, and how can we extend the model for further insight in future studies? We discuss several possible avenues below.

Evolutionary dynamics at the center of origin of ring species remain understudied (see also Kuchta and Wake 2016). Because ancestral area populations are by default oldest in the system, standard biogeographic predictions would include high genetic diversity and perhaps ancestral introgression, as in *Calisoga* (fig. 4*D*). In an example of ephemeral ring species in *Sceloporus* lizards, Bouzid et al. (2022) note high genetic diversity in the ancestral area, reflecting longer-term stability. One might hypothesize that increased ancestral genomic variation would impact the genomic path of speciation (Pease et al. 2016; Marques et al. 2019), but to the best of our knowledge, this has not been studied or modeled for ring situations. Phylogenetic

predictions also remain unclear. One prediction might be ancestral area paraphyly, resulting from the sorting of ancestral genetic variation. Deep paraphyly is found in the inferred ancestral ranges for both mariposa lilies (Hernández et al. 2022) and in *Ensatina*. Alternatively, a primary phylogenetic split might be most expected in the ancestral area, as seen in *Calisoga*, although such a model then (perhaps paradoxically) becomes a two-lineage model. In slipper spurges, a primary phylogenetic split is found in the inferred ancestral area of Mexico and Guatemala (Cacho and Baum 2012). We emphasize that a tree-like model might be generally inappropriate for this ancestral area problem and that network methods might be better suited.

We view evolutionary age, lineage persistence, dispersal limitation, parapatry, and slow rates of reproductive isolation evolution as key and interconnected aspects of a broken ring model. In combination, these parameters are largely lacking from existing simulation studies of ring speciation. On the surface this combination seems empirically restrictive, but this cannot be more restrictive than an idealized model (for which basically no empirical examples exist) and might better be viewed as pointing toward particular geographic areas and taxa in which to further explore broken ring speciation. Taxa must have existed on landscapes long enough to experience biogeographic barriers but simultaneously have not experienced profound population extinction. For example, *Calisoga* and many other ground-dwelling taxa have natural history attributes that enhance persistence on the landscape, including constructing their own suitable microenvironments in underground burrows. Other taxa are known to have similar long-term evolutionary persistence (Mason et al. 2018; Jockusch et al. 2020). Combined with the above are dispersal distances that are small compared with the size of the barrier, allowing for time for buildup of reproductive isolation, which itself evolves relatively slowly. Kuchta and Wake (2016) discuss slowly evolving reproductive isolation in *Ensatina*, and we contend that this might represent an important general aspect of broken ring speciation.

Genetic clines are implicit in a ring species model, and a broken ring composed of numerous lineages can still lead to clinal variation. A key component of broken ring species is that lineages are not strictly allopatric in their distribution but have the potential over evolutionary time to contact and interact. Combined with spatial persistence, this geographical adjacency allows for sporadic gene flow (even at low levels) after divergence. These interactions are occurring at areas where neighboring lineages likely occupy similar environments. Similar ecological requirements and postdivergence gene flow would together help to inhibit ecological divergence among neighboring lineages around the ring. Importantly, the adjacent lineages at the terminus would have had no genetic interaction since initial divergence, and combined with older evolutionary ages and low dispersal, Dobzhansky-Muller incompatibilities (Orr and Turelli 2001) and/or other forms of reproductive isolation could create more absolute barriers at ring terminus. For example, given the age and dispersal limitation of *Calisoga*, by the time the two arms meet, they have been genetically separated for multiple millions of years.

Dynamics during long-term movements around the ring are also of central importance. In a broken ring model, ecological conditions near the origin may be similar for two lineages, and ecological conditions at ring closure would also be similar. But ecological conditions experienced along the journey are expected to differ between the two arms. These could include differences in predation pressures, climate, soils, and competition, which certainly exist between the northern and southern arms of *Calisoga*. Character displacement may contribute to morphological divergence of lineages in sympatry, but we hypothesize that ecological divergence had to evolve prior in order for coexistence. The difference in selective pressures along the different distributional arms is key to the absolute closure of the *Calisoga* system. In this sense, broken ring speciation (and ring speciation more generally) is not merely "speciation by distance" but rather depends on ecological differences experienced over the colonization routes. Also, with range expansion associated with ring closure, serial founder events could promote independent population bottlenecks and drift-driven divergence relative to the center of origin. Together, both natural selection and drift should contribute to the divergence of the two arms as they travel along different routes. Although many of the arguments above also apply to an idealized ring speciation model (Mayr 1942; Stebbins 1949; Irwin et al. 2001), key differences include the expected deeper evolutionary history of a broken system (also dependent on evolutionary persistence), with more evolutionary time allowing for ecological and landscape differences to accumulate.

Lineage adjacency and persistence also provide opportunities for studies of nonterminal contact, perhaps replicated in different parts of a broken ring, and comparisons with dynamics of terminal contact. This replication within the same system could be more powerful than a standard study of secondary contact, holding many variables constant (same system) while allowing dissection of key alternative parameters, such as time alone or time plus ecological divergence (Pereira and Wake 2009). Replication also provides the possibility to explore an age series of contacts, informing the pace of evolution of reproductive isolation (Singhal and Moritz 2013). In *Ensatina*, contact zones span a range of levels of reproductive isolation and showcase a

continuum of evolutionary possibilities, from genetic merger of adjacent lineages to complete reproductive isolation (Alexandrino et al. 2005; Pereira and Wake 2009; Pereira et al. 2011). Greenish warblers (*Phylloscopus*) also reveal a nonterminal contact with higher levels of genetic exchange than seen at terminal contact, providing important context for the latter (Alcaide et al. 2014). In *Calisoga*, Leavitt et al. (2015) found two locations in the Sierra Nevada foothills where limited sampling suggested lineage contact, in lineage pairs that differ in levels of phylogenomic divergence (Coulter vs. centSier within the South clade; Calaveras vs. noSier, representing South vs. North clades). Morphological differentiation between these lineage pairs is modest in comparison to that seen at terminal overlap (fig. 6*C*); future tests of gene flow at these locations, including focused sampling and larger sample sizes, would be informative.

Conclusion

Ensatina and *Calisoga* are small, dispersal limited animals living in an expansive landscape. *Ensatina* is perhaps twice the evolutionary age of *Calisoga* and, as suggested by some authors (Kuchta and Wake 2016), has likely been "broken and reassembled" multiple times. Despite this age and ubiquitous genetic fragmentation, *Ensatina* retains many features of a broken ring model and is one of a handful of textbook examples of this pattern and process. Our fundamental contention is that *Calisoga* can be characterized as a broken ring species as well as *Ensatina* can. *Calisoga* has high potential as a study model, and we hope that our results spur more interest in this system and in further theoretical and empirical exploration of a broken ring speciation model.

Acknowledgments

Many people helped to collect specimens, including J. Bond, B. Boyer, S. Castillo, L. Chamberland, E. Ciaccio, S. Derkarabetian, R. Fitch, E. Garcia, R. W. Mendez, L. Newton, A. Rivera, J. Satler, A. Schoenhofer, D. Sitzmann, E. Stivers, Z. Thompson, and others listed in Leavitt et al. (2015). J. Bond provided ultraconserved element data for several out-group taxa. E. Stivers and L. Irons helped to measure specimens and extract DNA. Guilherme Azevedo provided assistance with bioinformatic tools. A grant from the National Science Foundation (DEB1937725 to M.H. and J. Bond) funded this research. R.M.-R. was supported by the National Science Foundation and a Consejo Nacional de Ciencia y Tecnología postdoctoral grant (770665/800981). Comments from E. Jochim helped to improve the manuscript; the manuscript was greatly strengthened during the rigorous and highly constructive review process led by S. Singhal and two anonymous reviewers.

Statement of Authorship

R.M.-R. and M.H. conceptualized the project; M.H. acquired funding; R.M.-R. and M.H. developed methods and the experimental design; R.M.-R., M.H., J.S., and D.L. collected data; R.M.-R. analyzed and visualized the data; R.M.-R. and M.H. wrote the original draft; and R.M.-R., M.H., J.S., and D.L. reviewed and edited the draft.

Data and Code Availability

Data and code have been deposited in the Dryad Digital Repository (https://doi.org/10.5061/dryad.70rxwdc47, Monjaraz-Ruedas et al. 2024) and GenBank Sequence Read Archive repository (BioProject PRJNA1073270).

Literature Cited

Ackerly, D. D. 2009. Evolution, origin and age of lineages in the Californian and Mediterranean floras. Journal of Biogeography 36:1221–1233.

Alcaide, M., E. S. C. Scordato, T. D. Price, and D. E. Irwin. 2014. Genomic divergence in a ring species complex. Nature 511:83–85.

Alexandrino, J., S. J. E. Baird, L. Lawson, J. R. Macey, C. Moritz, and D. B. Wake. 2005. Strong selection against hybrids at a hybrid zone in the *Ensatina* ring species complex and its evolutionary implications. Evolution 59:1334–1347.

Axelrod, D. I. 1973. History of the Mediterranean ecosystem in California. Pages 225–277 *in* Mediterranean type ecosystems: origin and structure. Springer, Berlin.

Baldwin, B. G., A. H. Thornhill, W. A. Freyman, D. D. Ackerly, M. M. Kling, N. Morueta-Holme, and B. D. Mishler. 2017. Species richness and endemism in the native flora of California. American Journal of Botany 104:487–501.

Benjamini, Y., and Y. Hochberg. 1995. Controlling the false discovery rate: a practical and powerful approach to multiple testing. Journal of the Royal Statistical Society B 57:289–300.

Bentzien, M. M. 1976. The biosystematics of the spider genus *Brachythele* Ausserer (Araneidae: Dipluridae). PhD diss. University of California, Berkeley.

Bolger, A. M., M. Lohse, and B. Usadel. 2014. Trimmomatic: a flexible trimmer for Illumina sequence data. Bioinformatics 30:2114–2120.

Bond, J. E., D. A. Beamer, T. Lamb, and M. Hedin. 2006. Combining genetic and geospatial analyses to infer population extinction in mygalomorph spiders endemic to the Los Angeles region. Animal Conservation 9:145–157.

Bouzid, N. M., J. W. Archie, R. A. Anderson, J. A. Grummer, and A. D. Leaché. 2022. Evidence for ephemeral ring species formation during the diversification history of western fence lizards (*Sceloporus occidentalis*). Molecular Ecology 31:620–631.

Bowersox, J. R. 2005. Reassessment of extinction patterns of Pliocene molluscs from California and environmental forcing of extinction in the San Joaquin Basin. Palaeogeography, Palaeoclimatology, Palaeoecology 221:55–82.

Buckett, J. S., and M. R. Gardner. 1969. A review of the genus *Gosodesmus* Chamberlin, with the synonymy of *Eucybe* Chamberlin (Diplopoda: Platydesmida: Andrognathidae). Journal of the New York Entomological Society 1969:40–50.

Burge, D. O., J. H. Thorne, S. P. Harrison, B. C. O'Brien, J. P. Rebman, J. R. Shevock, E. R. Alverson, et al. 2016. Plant diversity and endemism in the California Floristic Province. Modroño 63:3–206.

Cacho, I. N., and D. A. Baum. 2012. The Caribbean slipper spurge *Euphorbia tithymaloides*: the first example of a ring species in plants. Proceedings of the Royal Society B 279:3377–3383.

Castresana, J. 2000. Selection of conserved blocks from multiple alignments for their use in phylogenetic analysis. Molecular Biology and Evolution 17:540–552.

Caye, K., T. M. Deist, H. Martins, O. Michel, and O. François. 2016. TESS3: fast inference of spatial population structure and genome scans for selection. Molecular Ecology Resources 16:540–548.

Cazier, M. A. 1942. A monographic revision of the genus *Omus* (Coleoptera-Cicindelidae). PhD diss. University of California, Berkeley.

Chang, C. C., C. C. Chow, L. C. A. M. Tellier, S. Vattikuti, S. M. Purcell, and J. J. Lee. 2015. Second-generation PLINK: rising to the challenge of larger and richer datasets. GigaScience 4:1–16.

Danecek, P., A. Auton, G. Abecasis, C. A. Albers, E. Banks, M. A. DePristo, R. E. Handsaker, et al. 2011. The variant call format and VCFtools. Bioinformatics 27:2156–2158.

Danecek, P., J. K. Bonfield, J. Liddle, J. Marshall, V. Ohan, M. O. Pollard, A. Whitwham, et al. 2021. Twelve years of SAMtools and BCFtools. GigaScience 10:1–4.

Dupre, W. R. 1990. Quaternary geology of the Monterey Bay region, California. Pages 185–191 *in* R. E. Garrison, H. G. Greene, K. R. Hicks, G. E. Weber, and T. L. Wright, eds. Geology and tectonics of the central California coastal region, San Francisco to Monterey. Pacific Section of the American Association of Petroleum Geologists, Bakersfield, CA.

Faircloth, B. C. 2016. PHYLUCE is a software package for the analysis of conserved genomic loci. Bioinformatics 32:786–788.

Flouri, T., B. Rannala, and Z. Yang. 2020. A tutorial on the use of BPP for species tree estimation and species delimitation. Pages 5.6:1–5.6:16 *in* C. Scornavacca, F. Delsuc, and N. Galtier, eds. Phylogenetics in the genomic era. HAL.

Frichot, E., and O. François. 2015. LEA: an R package for landscape and ecological association studies. Methods in Ecology and Evolution 6:925–929.

Frichot, E., F. Mathieu, T. Trouillon, G. Bouchard, and O. François. 2014. Fast and efficient estimation of individual ancestry coefficients. Genetics 196:973–983.

Furlong, K. P., and S. Y. Schwartz. 2004. Influence of the Mendocino triple junction on the tectonics of coastal California. Annual Review of Earth and Planetary Sciences 32:403–433.

Gruber, B., P. J. Unmack, O. F. Berry, and A. Georges. 2018. dartr: an R package to facilitate analysis of SNP data generated from reduced representation genome sequencing. Molecular Ecology Resources 18:691–699.

Hall, R. 2002. Cenozoic geological and plate tectonic evolution of SE Asia and the SW Pacific: computer-based reconstructions, model and animations. Journal of Asian Earth Sciences 20:353–431.

Harden, D. R. 1998. California geology. Prentice Hall, Upper Saddle River, NJ.

Harvey, M. S., B. Y. Main, M. G. Rix, and S. J. B. Cooper. 2015. Refugia within refugia: in situ speciation and conservation of threatened *Bertmainius* (Araneae: Migidae), a new genus of relictual trapdoor spiders endemic to the mesic zone of southwestern Australia. Invertebrate Systematics 29:511–553.

Hernández, A. I., J. B. Landis, and C. D. Specht. 2022. Phylogeography and population genetics reveal ring species patterns in a highly polymorphic California lily. Journal of Biogeography 49:416–430.

Hoang, D. T., O. Chernomor, A. von Haeseler, B. Q. Minh, and L. S. Vinh. 2018. UFBoot2: improving the ultrafast bootstrap approximation. Molecular Biology and Evolution 35:518–522.

Irwin, D. E., J. H. Irwin, and T. D. Price. 2001. Ring species as bridges between microevolution and speciation. Genetica 112/113:223–243.

Irwin, D. E., and D. B. Wake. 2016. Ring species. Pages 467–475 *in* R. M. Kliman, ed. Encyclopedia of evolutionary biology. Academic Press, Oxford.

Jackman, T. R., and D. B. Wake. 1994. Evolutionary and historical analysis of protein variation in the blotched forms of salamanders of the *Ensatina* complex (Amphibia: Plethodontidae). Evolution 48:876–897.

Jockusch, E. L., R. W. Hansen, R. N. Fisher, and D. B. Wake. 2020. Slender salamanders (genus *Batrachoseps*) reveal Southern California to be a center for the diversification, persistence, and introduction of salamander lineages. PeerJ 8:e9599.

Jombart, T. 2008. adegenet: a R package for the multivariate analysis of genetic markers. Bioinformatics 24:1403–1405.

Jombart, T., and I. Ahmed. 2011. adegenet 1.3–1: new tools for the analysis of genome-wide SNP data. Bioinformatics 27:3070–3071.

Joseph, L., G. Dolman, S. Donnellan, K. M. Saint, M. L. Berg, and A. T. D. Bennett. 2008. Where and when does a ring start and end? testing the ring-species hypothesis in a species complex of Australian parrots. Proceedings of the Royal Society B 275:2431–2440.

Kalyaanamoorthy, S., B. Q. Minh, T. K. F. Wong, A. Von Haeseler, and L. S. Jermiin. 2017. ModelFinder: fast model selection for accurate phylogenetic estimates. Nature Methods 14:587–589.

Katoh, K., G. Asimenos, and H. Toh. 2009. Multiple alignment of DNA sequences with MAFFT. Methods in Molecular Biology 537:39–64.

Kuchta, S. R., D. S. Parks, R. L. Mueller, and D. B. Wake. 2009. Closing the ring: historical biogeography of the salamander ring species *Ensatina eschscholtzii*. Journal of Biogeography 36:982–995.

Kuchta, S. R., and A. M. Tan. 2006. Lineage diversification on an evolving landscape: phylogeography of the California newt, *Taricha torosa* (Caudata: Salamandridae). Biological Journal of the Linnean Society 89:213–239.

Kuchta, S. R., and D. B. Wake. 2016. Wherefore and whither the ring species? Copeia 104:189–201.

Lancaster, L. T., and K. M. Kay. 2013. Origin and diversification of the California flora: re-examining classic hypotheses with molecular phylogenies. Evolution 67:1041–1054.

Lanfear, R., and M. Hahn. 2024. The meaning and measure of concordance factors in phylogenomics. Eco Evo Rxiv, https://doi.org/10.32942/X27617.

Lê, S., J. Josse, and F. Husson. 2008. FactoMineR: an R package for multivariate analysis. Journal of Statistical Software 25:1–18.

Leavitt, D. H., J. Starrett, M. F. Westphal, and M. Hedin. 2015. Multilocus sequence data reveal dozens of putative cryptic species in a radiation of endemic Californian mygalomorph spiders (Araneae, Mygalomorphae, Nemesiidae). Molecular Phylogenetics and Evolution 91:56–67.

Li, H. 2013. Aligning sequence reads, clone sequences and assembly contigs with BWA-MEM. arXiv, https://doi.org/10.48550/arXiv.1303.3997.

Malinsky, M., M. Matschiner, and H. Svardal. 2021. Dsuite: fast D-statistics and related admixture evidence from VCF files. Molecular Ecology Resources 21:584–595.

Marcus, J., W. Ha, R. F. Barber, and J. Novembre. 2021. Fast and flexible estimation of effective migration surfaces. eLife 10:1–46.

Marques, D. A., J. I. Meier, and O. Seehausen. 2019. A combinatorial view on speciation and adaptive radiation. Trends in Ecology and Evolution 34:531–544.

Martins, A. B., M. A. M. De Aguiar, and Y. Bar-Yam. 2013. Evolution and stability of ring species. Proceedings of the National Academy of Sciences of the USA 110:5080–5084.

Mason, L. D., G. Wardell-Johnson, and B. Y. Main. 2018. The longest-lived spider: mygalomorphs dig deep, and persevere. Pacific Conservation Biology 24:203–206.

Mason, N. A., N. K. Fletcher, B. A. Gill, W. C. Funk, and K. R. Zamudio. 2020. Coalescent-based species delimitation is sensitive to geographic sampling and isolation by distance. Systematics and Biodiversity 18:269–280.

Matzke, N. J. 2014. Model selection in historical biogeography reveals that founder-event speciation is a crucial process in island clades. Systematic Biology 63:951–970.

Mayr, E. 1942. Systematics and the origin of species. Columbia University Press, New York.

Minh, B. Q., M. W. Hahn, and R. Lanfear. 2020*a*. New methods to calculate concordance factors for phylogenomic datasets. Molecular Biology and Evolution 37:2727–2733.

Minh, B. Q., H. A. Schmidt, O. Chernomor, D. Schrempf, M. D. Woodhams, A. Von Haeseler, R. Lanfear, et al. 2020*b*. IQ-TREE 2: new models and efficient methods for phylogenetic inference in the genomic era. Molecular Biology and Evolution 37:1530–1534.

Mirarab, S., and T. Warnow. 2015. ASTRAL-II: coalescent-based species tree estimation with many hundreds of taxa and thousands of genes. Bioinformatics 31:i44–i52.

Monahan, W. B., R. J. Pereira, and D. B. Wake. 2012. Ring distributions leading to species formation: a global topographic analysis of geographic barriers associated with ring species. BMC Biology 10:20.

Monjaraz-Ruedas, R., J. Starrett, D. Leavitt, and M. Hedin. 2024. Data from: Broken ring speciation in California mygalomorph spiders (Nemesiidae, *Calisoga*). American Naturalist, Dryad Digital Repository, https://doi.org/10.5061/dryad.70rxwdc47.

Moritz, C., C. J. Schneider, and D. B. Wake. 1992. Evolutionary relationships within the *Ensatina eschscholtzii* complex confirm the ring species interpretation. Systematic Biology 41:273–291.

Orr, H. A., and M. Turelli. 2001. The evolution of postzygotic isolation: accumulating Dobzhansky-Muller incompatibilities. Evolution 55:1085–1094.

Patterson, N., P. Moorjani, Y. Luo, S. Mallick, N. Rohland, Y. Zhan, T. Genschoreck, et al. 2012. Ancient admixture in human history. Genetics 192:1065–1093.

Pease, J. B., D. C. Haak, M. W. Hahn, and L. C. Moyle. 2016. Phylogenomics reveals three sources of adaptive variation during a rapid radiation. PLoS Biology 14:e1002379.

Pereira, R. J., W. B. Monahan, and D. B. Wake. 2011. Predictors for reproductive isolation in a ring species complex following genetic and ecological divergence. BMC Evolutionary Biology 11:194.

Pereira, R. J., and D. B. Wake. 2009. Genetic leakage after adaptive and nonadaptive divergence in the *Ensatina eschscholtzii* ring species. Evolution 63:2288–2301.

Platnick, N. I., and D. Ubick. 2008. A revision of the endemic Californian spider genus *Titiotus* Simon (Araneae, Tengellidae). American Museum Novitates 2008:1–34.

Powell, C. L., J. A. Barron, A. M. Sarna-Wojcicki, J. C. Clark, F. A. Perry, E. E. Brabb, and R. J. Fleck. 2007. Age, stratigraphy, and correlations of the late Neogene Purisima Formation, central California Coast Ranges. US Geological Survey Professional Paper 1740:1–32.

Prjibelski, A., D. Antipov, D. Meleshko, A. Lapidus, and A. Korobeynikov. 2020. Using SPAdes de novo assembler. Current Protocols in Bioinformatics 70:1–29.

Rabiee, M., E. Sayyari, and S. Mirarab. 2019. Multi-allele species reconstruction using ASTRAL. Molecular Phylogenetics and Evolution 130:286–296.

Ree, R. H., and S. A. Smith. 2008. Maximum likelihood inference of geographic range evolution by dispersal, local extinction, and cladogenesis. Systematic Biology 57:4–14.

Rix, M. G., J. A. Huey, B. Y. Main, J. M. Waldock, S. E. Harrison, S. Comer, A. D. Austin, and M. S. Harvey. 2017. Where have all the spiders gone? the decline of a poorly known invertebrate fauna in the agricultural and arid zones of southern Australia. Austral Entomology 56:14–22.

Rubinoff, D., C. Doorenweerd, J. S. McElfresh, and J. G. Millar. 2021. Phylogeography of an endemic California silk moth genus suggests the importance of an unheralded central California province in generating regional endemic biodiversity. Molecular Phylogenetics and Evolution 164:107256.

Satler, J. D., B. C. Carstens, and M. Hedin. 2013. Multilocus species delimitation in a complex of morphologically conserved trapdoor spiders (Mygalomorphae, Antrodiaetidae, *Aliatypus*). Systematic Biology 62:805–823.

Sayyari, E., and S. Mirarab. 2016. Fast coalescent-based computation of local branch support from quartet frequencies. Molecular Biology and Evolution 33:1654–1668.

Schierenbeck, K. A. 2014. Phylogeography of California: an introduction. University of California Press, Berkeley.

Singhal, S., and C. Moritz. 2013. Reproductive isolation between phylogeographic lineages scales with divergence. Proceedings of the Royal Society B 280:20132246.

Stange, M., M. R. Sánchez-Villagra, W. Salzburger, and M. Matschiner. 2018. Bayesian divergence-time estimation with genome-wide single-nucleotide polymorphism data of sea catfishes (Ariidae) supports Miocene closure of the Panamanian Isthmus. Systematic Biology 67:681–699.

Staub, N. L., C. W. Brown, and D. B. Wake. 1995. Patterns of growth and movements in a population of *Ensatina eschscholtzii platensis* (Caudata: Plethodontidae) in the Sierra Nevada, California. Journal of Herpetology 29:593–599.

Stebbins, R. C. 1949. Speciation in salamanders of the plethodontid genus *Ensatina*. University of California Publications in Zoology 48:377–526.

Stoltz, M., B. Baeumer, R. Bouckaert, C. Fox, G. Hiscott, and D. Bryant. 2021. Bayesian inference of species trees using diffusion models. Systematic Biology 70:145–161.

Sukumaran, J., and L. L. Knowles. 2017. Multispecies coalescent delimits structure, not species. Proceedings of the National Academy of Sciences of the USA 114:1607–1612.

Tumescheit, C., A. E. Firth, and K. Brown. 2022. CIAlign: a highly customisable command line tool to clean, interpret and visualise multiple sequence alignments. PeerJ 10:e12983.

Ubick, D., and J. M. Ledford. 2005. Nemesiidae. Pages 60–61 *in* D. Ubik, P. Paquin, P. E. Cushing, and V. Roth, eds. Spiders of North America: an identification manual. American Arachnological Society, Poughkeepsie, NY.

Wake, D. B. 1997. Incipient species formation in salamanders of the *Ensatina* complex. Proceedings of the National Academy of Sciences of the USA 94:7761–7767.

Wake, D. B., and K. P. Yanev. 1986. Geographic variation in allozymes in a "ring species", the plethodontid salamander *Ensatina eschscholtzii* of western North America. Evolution 40:702–715.

Wang, Y., A. Feijó, J. Cheng, L. Xia, Z. Wen, D. Ge, J. Sun, et al. 2021. Ring distribution patterns—diversification or speciation? comparative phylogeography of two small mammals in the mountains surrounding the Sichuan Basin. Molecular Ecology 30:2641–2658.

Yang, Z., and B. Rannala. 2010. Bayesian species delimitation using multilocus sequence data. Proceedings of the National Academy of Sciences of the USA 107:9264–9269.

———. 2014. Unguided species delimitation using DNA sequence data from multiple loci. Molecular Biology and Evolution 31:3125–3135.

Zarza, E., E. M. Connors, J. M. Maley, W. L. E. Tsai, P. Heimes, M. Kaplan, and J. E. McCormack. 2018. Combining ultraconserved elements and mtDNA data to uncover lineage diversity in a Mexican highland frog (Sarcohyla; Hylidae). PeerJ 6:e6045.

Zhang, C., M. Rabiee, E. Sayyari, and S. Mirarab. 2018. ASTRAL-III: polynomial time species tree reconstruction from partially resolved gene trees. BMC Bioinformatics 19:15–30.

References Cited Only in the Online Enhancements

Barnes, R., and K. Sahr. 2017. dggridR: discrete global grids for R. https://CRAN.R-project.org/package=dggridR.

Bouckaert, R., J. Heled, D. Kühnert, T. Vaughan, C. H. Wu, D. Xie, M. A. Suchard, et al. 2014. BEAST 2: a software platform for Bayesian evolutionary analysis. PLoS Computational Biology 10:e1003537.

Goudet, J. 2005. HIERFSTAT, a package for R to compute and test hierarchical *F*-statistics. Molecular Ecology Notes 5:184–186.

Junier, T., and E. M. Zdobnov. 2010. The Newick utilities: high-throughput phylogenetic tree processing in the UNIX shell. Bioinformatics 26:1669–1670.

Knaus, B. J., and N. J. Grünwald. 2017. vcfr: a package to manipulate and visualize variant call format data in R. Molecular Ecology Resources 17:44–53.

Kulkarni, S., H. Wood, M. Lloyd, and G. Hormiga. 2020. Spider-specific probe set for ultraconserved elements offers new perspectives on the evolutionary history of spiders (Arachnida, Araneae). Molecular Ecology Resources 20:185–203.

Maddison, W. P., I. Beattie, K. Marathe, P. Y. C. Ng, N. Kanesharatnam, S. P. Benjamin, and K. Kunte. 2020. A phylogenetic and taxonomic review of Baviine jumping spiders (Araneae, Salticidae, Baviini). ZooKeys 2020:27–97.

Mai, U., and S. Mirarab. 2018. TreeShrink: fast and accurate detection of outlier long branches in collections of phylogenetic trees. BMC Genomics 19:272.

Opatova, V., C. A. Hamilton, M. Hedin, L. M. De Oca, J. Král, J. E. Bond, and B. Wiegmann. 2020. Phylogenetic systematics and evolution of the spider infraorder Mygalomorphae using genomic scale data. Systematic Biology 69:671–707.

Rambaut, A., A. J. Drummond, D. Xie, G. Baele, and M. A. Suchard. 2018. Posterior summarization in Bayesian phylogenetics using Tracer 1.7. Systematic Biology 67:901–904.

Starrett, J., S. Derkarabetian, M. Hedin, R. W. Bryson, J. E. McCormack, and B. C. Faircloth. 2017. High phylogenetic utility of an ultraconserved element probe set designed for Arachnida. Molecular Ecology Resources 17:812–823.

van Etten, J. 2017. R package gdistance: distances and routes on geographical grids. Journal of Statistical Software 76:1–21.

Associate Editor: Sonal Singhal
Editor: Jill T. Anderson

Adult female of the mygalomorph spider genus *Calisoga*, family Nemesiidae. Photo credit: Marshal Hedin.